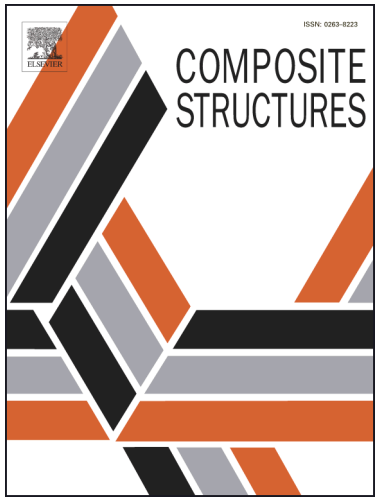

Effect of distance between impact point and hole position on the impact fatigue strength of composite laminates

R.A.M. Santos, P.N.B. Reis, M.J. Santos, C.A.C.P. Coelho

PII: S0263-8223(16)32199-7
DOI: http://dx.doi.org/10.1016/j.compstruct.2017.02.045
Reference: COST 8266

To appear in: *Composite Structures*

Received Date: 17 October 2016
Revised Date: 19 December 2016
Accepted Date: 10 February 2017

Please cite this article as: Santos, R.A.M., Reis, P.N.B., Santos, M.J., Coelho, C.A.C.P., Effect of distance between impact point and hole position on the impact fatigue strength of composite laminates, *Composite Structures* (2017), doi: http://dx.doi.org/10.1016/j.compstruct.2017.02.045

Effect of distance between impact point and hole position on the impact fatigue strength of composite laminates

R.A.M. Santos[1], P.N.B. Reis[2], M.J. Santos[3], C.A.C.P. Coelho[4]

[1] Depart. of Aerospace Sciences, University of Beira Interior, Covilhã, Portugal

[2)] Depart. of Electromechanical Engineering, University of Beira Interior, Covilhã, Portugal

[3)] CEMUC, Depart. of Electrical and Computers Engineering, University of Coimbra, Coimbra, Portugal

[4)] ESTA, Escola Superior de Tecnologia de Abrantes, Instituto Politécnico de Tomar, Tomar, Portugal

Abstract

An impact fatigue study was performed to evaluate the effect of the distance between the impact point and the hole on the fatigue life of glass fibre/epoxy laminates. For this purpose, experimental tests were carried out in square plates and for the distances of 0, 5, 10 and 20 mm, from the impact point. The results were compared with the ones obtained in plates without hole. It was possible to conclude that **the fatigue life decreased, comparatively to the control samples, about 10.9%, 40%, 63.6% and 69.1% for the distances of 20 mm, 10 mm, 5 mm and 0 mm, respectively.** Higher distances promote higher maximum loads and elastic restitution, but an opposite trend in terms of maximum displacement. **For example, it was found for 20 mm a maximum load around 5.54 kN, a displacement of about 4.4 mm and an elastic energy of 59.2%, while for 0 mm these values were about 4.59 kN, 5.7 mm and 40.4%, respectively.** In terms of multi-impacts, the damage severity is also very influenced by the distance. For small distances the damage progresses quickly, while three stages can be found for the control samples and for the distance of 20 mm.

Keywords: Composites; Impact strength; Mechanical characterization; Holes.

1. INTRODUCTION

It is recognised that, in many cases, the structural application of composite materials requires open holes to allow the access of electric wires, hydraulic pipes, assembly and/or maintenance activities. In this context, damage will initiate and grow from these notches, due to the stress/strain concentrations, with consequent lower strength and/or life.

However, the sensitivity of a composite laminate to a notch shows to be dependent on a large number of parameters, such as laminate size and thickness, notch size and geometry, width/diameter ratios, ply orientation and thickness, machining quality and material properties [1-3]. All of these factors affect the mechanical properties by changing the extent of damage growth during loading, and interact with each other to enhance the individual effects [1]. For example, in terms of woven fabric composites with holes, the magnitude and severity of strain concentration is strongly influenced by the tensile loading direction, hole geometry and its dimension relative to the unit cell of the plain woven fabrics [4, 5]. On the other hand, for 3D woven carbon/epoxy composites, the notched tensile strength is less than 17% lower than the un-notched tensile strength and it is not very sensitive to the notch size [6]. For these laminates, the fractured notched samples showed similar failure modes as the un-notched samples, such as warp tow fracture, debonding and matrix cracking [6]. Four different stacking sequences were studied by Achard *et al*. [7], where the importance of the position of 0º plies in the thickness of the laminate was analysed. Authors demonstrated that the 0º plies placed near or at the outer surface split more easily, so the stress concentration near the hole diminished and the final failure was delayed. Therefore, according to the authors, the 0º plies are protected inside the laminate [7]. On the other hand, the general patterns of damage of 45º and 90º plies adjacent to 0º plies were generally quite similar, with a difference only when the 0º plies split. In this case, the local stress fields were modified. Matrix cracking in a ply always occurred before delamination at adjacent interfaces, similar to those identified in impact [7]. Green *et al*. [1] investigated the effect of scaling on the tensile strength of notched composites. Hole diameter, ply and laminate thickness, were studied as the independent variables, whilst keeping constant ratios of hole diameter to width and length, over a scaling range of 8 from the baseline size. In general it was observed

that the strength decreased when the specimen size increasing (with a maximum reduction around 64%), however, the reverse trend of strength increasing with in-plane dimensions was found for specimens with plies blocked together. Three distinct failure mechanisms were observed: fibre failure with and without extensive matrix damage, and complete gauge section delamination [1]. Finally, Zitoune *et al*. [8] compared two categories of perforated specimens loaded in tension. The holes of the first category are obtained by drilling and by moulding for the second category. The tensile strength for moulded hole specimens is higher or equal to 30% than those obtained for drilled hole specimens. It was observed different damage mechanisms between drilled holes and moulded holes specimens, and the strain fields showed that the maximum deformation of drilled hole is twice as high compared to those of moulded hole [8].

The effect of size on the strength of composite laminates with central holes loaded in tension and compression was studied by Erçin *et al*. [3]. Specimens presented different hole sizes but with constant width-to-diameter ratios. The open-hole tensile strength was 66-91% higher than the open hole compression strength, being the difference more pronounced for the specimens with the largest dimensions. The detrimental effect of reversing the load from tension to compression is more pronounced in the notched specimens. Comparing the unnotched tensile and compressive strengths, the strength reduction resulting from applying a compressive load is only 48% [3].

Waas and Babcock [9] studied the compressive failure in graphite-epoxy laminates containing a single hole. They observed that damage initiates by a combination of fibre microbuckling and delamination. The 0º ply microbuckling originates at the hole edges at 80% of the ultimate compressive strength and propagates into the interior of the specimen. The in-plane compressive fracture behaviour of carbon fibre-epoxy multidirectional laminates containing a single hole was studied by Soutis and Fleck [10], and they reported up to 40% reduction in the compressive strength. The dominant failure was fibre microbuckling in the 0º plies [10]. The compressive behaviour of the pultruded composite plate specimens with and without holes was investigated by Saha *et al*. [11]. A wide range of hole diameter to width ratios was analysed to determine the compressive strength as a function of hole size. The strain at

the hole edge increases with the increasing of hole diameter, and the compressive strength was found to be higher for 6.3 mm than the value observed for 12.7 mm thick. The post failure analysis suggested that the compressive failure mechanisms consist of delamination, fibre microbuckling and shearing of continuous strand mats layers [11]. The compressive failure mechanism of quasi-isotropic composite laminates with an open hole was studied by Suemasu *et al*. [12]. Two types of composite systems were investigated to examine the dependence of failure behaviour on the material properties (such as interlaminar toughness). Independently of the laminate, the first damage was fibre micro-buckling in the 0º layer. Some accumulation of damage, such as further fibre micro-buckling in the 0º layers and interlaminar delaminations in several interfaces, was observed before the final unstable fracture in the laminate with high interlaminar toughness, while sudden failure occurred in the laminate with low interlaminar toughness [12].

If the effect of holes or cut-outs has been studied extensively in terms of tensile and compressive behaviour, there are very few works related with impacts at low velocity [13]. This mode of loading is very dangerous, because it promotes damages very difficult to detect [14, 15] and, simultaneously, the residual properties of the composite materials are significantly affected [16-20].

In this context, Green *et al*. [21] reported the first results of an experimental and numerical study to determine the additional damage arising from the presence of holes. They are responsible by the matrix cracks that occur in the lower lamina, and these multiple cracks can extend from the region directly below the impact to the edge of the holes. In some circumstances, further cracks can emanate from the far side of the holes. Studies performed by Luo [22] show that, in composites with open holes, the damage consists basically in delamination associated with matrix crack, but with absence of fibre breakage. Two parallel matrix cracks appear between the impact point and the hole. One crack initiates at the point of impact and propagates towards the hole whereas the other crack initiates near the hole edge and propagates towards the impact centre. These cracks can be initiated by either tension or shear or a combination of both. On the other hand, when the laminates contain two holes, Roy and Chakraborty [13] found that the delaminations initiate at the interface from the inner free edges of the

holes and with time, they meet each other forming a big delamination area. Finally, Amaro *et al*. [23] found that the failure morphology is altered by the presence of holes, confirming a complex damage mechanism (interaction between matrix cracking and delamination).

In terms of impact **fatigue** strength, for the knowledge of the authors, literature does not report any study about the topic of the present work, because all **of them are** essentially oriented to characterize, by experimental and numerical procedures, the additional damage arising from the presence of holes and respective damage mechanisms. Therefore, the main goal of the present work is to analyse the effect of distance between impact point and hole position **on the fatigue life** of glass fibre/epoxy laminates. The results will be discussed in terms of load-time, load-displacement, energy-time diagrams and evaluation of the damage.

2. MATERIALS AND PROCEDURE

Eight ply laminates, all in the same direction, of woven bi-directional glass fibre 1195P (195 g/m^2), were prepared by hand lay-up and the overall dimensions of the plates were 330x330x3 [mm]. Biresin® CR122 epoxy resin and a Biresin® CH122-3 hardener, supplied by Sika, were used. The system was placed inside a vacuum bag and a load of 2.5 kN was applied for 12 hours in order to maintain a constant fibre volume fraction and uniform laminate thickness. During the first 4 hours the bag remained attached to a vacuum pump to eliminate any air bubbles existing in the composite. The post-cure was followed according to the manufacturer`s datasheet (epoxy resin) in an oven at 60 ºC for 8 hours.

The samples used in the experiments were cut from those thin plates to square specimens with 100 mm side (100x100x3 mm). In these samples, using a special drill, open holes with 4 mm of diameter and centred with distances of 0, 5, 10 and 20 mm from the geometric centre were introduced, as shows Figure 1. **The specimens were machined under dry cutting conditions with a feed rate of 0.04 mm/rev using a solid carbide twist drill from M.A. Ford®, model EDF27127, with diameter of 4 mm, 54 mm long and two cutting edges. The drill and machining parameters were selected based**

on the study developed by Abrão *et al*. [24], taking into account the smallest damage obtained on similar laminates. On the other hand, the delamination size shows to be very dependent on the drill diameter [25], therefore, a diameter of 4 mm was chosen to minimize the damage size and considering the impactor diameter.

FIGURE 1

Low-velocity impact tests were performed using a drop weight-testing machine, IMATEK-IM10. More details about the impact machine can be found in [**26**]. An impactor with a diameter of 10 mm and mass of 2.827 kg was used. The tests were performed on square section samples of 75x75 mm and the impactor stroke at the centre of the samples obtained by centrally clamping the 100x100 mm specimens. The impact energy used in the tests was 12 J. This energy was previously selected in order to enable the measuring of the damage area, but without promoting perforation of the specimens. For each condition, three specimens were tested at room temperature and subjected to multi-impacts until full perforation occurs. Full perforation (FP) is defined when the impactor completely moves through the samples.

After impact tests, all the specimens were inspected in order to evaluate the size and shape of the damage. As the glass-laminated plates are translucent it is possible to obtain the image of the damage using photography. To achieve the best possible definition of the damaged area, the plates were photographed in counter-light using a powerful light source. Plates were framed in a window so that all the light could fall upon them. Simultaneously, the specimens were inspected by ultrasonic C-scan technique. For the ultrasonic analysis a 20 MHz broadband immersion piezocomposite transducer was used in the pulse-echo mode. The same transducer receives the echoes originated by multiple reflections inside the specimens from a longitudinal normal incident wave.

3. RESULTS AND DISCUSSION

Laminates with open holes were subjected to impact tests, in order to evaluate the distance effect between the impact point and the hole. Representative load-time and energy-time curves of all tests are

shown in Figure 2, and they are in good agreement with the literature [13, 23, **26-28**]. While Figure 2a represents the different curves obtained for the first impact on control samples and for the distances of 10 mm and 0 mm, Figure 2b shows the typical evolution of the curves for the control samples subjected to multi-impacts. These curves contain oscillations as consequence of the vibrations promoted by the samples [**27, 29, 30**].

FIGURE 2

The load-time curves are characterized by an increase in the load up to a maximum value (P_{max}) followed by a drop corresponding to the impactor rebound. The impact energy was not high enough to cause full penetration, because the impactor sticks into specimens and always rebounds. On the other hand, the beginning of the plateau corresponds to contact loss between the impactor and the specimen [**31, 32**]. Consequently, the difference between the maximum energy, corresponding to maximum load, and the energy defined by the plateau is the restitution component (elastic energy) due to impactor rebound. However, when the full perforation occurs (last impact), the elastic energy is zero because all energy is absorbed by the sample.

Table 1 presents the average values obtained for the first impact, and respective standard deviation, in terms of maximum load, maximum displacement and elastic recuperation. It is possible to observe that, higher distances promote an increasing of the maximum load and elastic recuperation. The highest maximum load is obtained for the control samples, around 5.9 kN, and this value decrease about 6.1%, 15.4%, 19% and 22.3% for the distances of 20 mm, 10 mm, 5 mm and 0 mm respectively. For the same comparison, in terms of elastic recuperation, reductions about 9.2%, 27.6%, 34.3% and 38.5% can be found, respectively. In this case, for the control samples, an average value around 65.7% was obtained. Finally, the maximum displacement presents an opposite tendency. With an average value of 4.1 mm for the control samples, this value increases around 7.7%, 21.6%, 28.9% and 37.7%, respectively, for the distances of 20 mm, 10 mm, 5 mm and 0 mm.

TABLE 1

From these results, and in terms of first impact, it is evident the effect of the distance on such

parameters, which is consequence of the damage promoted by the impact load on the samples. Figure 3 shows the damages obtained after the first impact for control samples and samples with the hole distanced 10 mm from the impact point. However, the damage mechanisms are representative of all configurations. Simultaneously, the damage was evaluated using two different techniques, photography in counter-light and ultrasonic C-scan technique.

FIGURE 3

Comparing the techniques, it is possible to conclude that both give a very precise detail of the damage outline and, in a global perspective, they are able to characterize the damage. However, these techniques produce only a two-dimensional view of the damage zone, giving no through-thickness data [15]. In fact all NDT approaches present limitations, and different techniques should be used in conjunction to evaluate the defects in terms of size and depth location.

From Figure 3, it is also possible to observe that the damage for the distance of 10 mm is smaller than the one observed for control samples. In fact the absence of holes (control samples) promotes a damage more spread by the laminate, while on the laminates with holes and distances of impact smaller than 10 mm the damage is more concentrated and it propagates in depth along the thickness. This is evident from the Table 1, where the displacements are much higher for distances shorter than 10 mm comparatively to the other ones. These damages are not evident by the technique used because, as referred previously, it is limited to a two-dimensional view.

In terms of damage mechanisms, **regardless of the machining parameters that have been selected to minimise the damages, it is expected some peel-up and push-out delaminations. However, according to Durão *et al*. [33] the push-out delaminations are more relevant because the peel-up dalaminations can be significantly minimised by reducing the feed rate, which was taken into account by the authors on the experimental procedure. On the other hand, in terms of impact loads,** matrix cracking is chronologically the first damaging mode [**34, 35**], which is followed by a rapid interlaminar fracture propagation. According to Green *et al*. [21], the matrix cracks occur in the lower lamina, and they will extend from the region directly below the impact to the edge of the holes. **As**

consequence of the push-out delaminations are located in the same region around the hole, further cracks can emanate from the side of the holes and, in these circumstances, two parallel matrix cracks appear between the impact point and the hole [22]. **One crack initiates at the point of impact and propagates towards the hole whereas the other one on the hole edge propagates towards the impact centre.** However, according to Pandita *et al*. [4], the failure starts at the location of the highest stress concentration and grows perpendicular to the loading direction, what can be determinant in this study for small distances. For higher distances the stress concentration is not **so** determinant, because, according Whitney and Nuismer [**36, 37**], it is assumed that failure occurs only when the stress at some distance away from the notch is equal to or greater than the unnotched laminate strength. Simultaneously to the stress concentration effect, the lower stiffness of the laminates, promoted by the hole, has also some influence on the impact parameters [**38**].

Figure 4 shows the effect of the distance between the impact point and the hole on the impact **fatigue** strength. **For this purpose, the results are plotted in terms of impact energy versus number of cycles to failure (N_f) curves, similar to the typical SN curves used on fatigue analysis.** Mean curve fitted to the experimental results is also superimposed. The laminates were considered failed, when full perforation occurs. Full perforation is defined when the impactor completely moves through the samples.

FIGURE 4

From the figure**, as expected,** it is possible to observe that the resistance of the laminates to repeated low velocity impacts shows to be very dependent on the distance between the impact point and the hole. In terms of average number of impacts to failure, and comparatively to the control samples, the **fatigue** life decreases about 10.9%, 40%, 63.6% and 69.1% for the distances of 20 mm, 10 mm, 5 mm and 0 mm, respectively.

The difference of lives observed above can be explained by the damage introduced. As discussed previously, its severity is highly dependent on the distance and this trend is also reproducible along the multi-impacts, as consequence of damage accumulation [**39**]. In this context, the impact bending

stiffness (IBS) is an important property to assess the damage progression in composite laminates subjected to multi-impacts [**40**], where, according to Amaro *et al*. [**41**], the damage can be directly correlated with the absorbed energy and inversely correlated with the impact bending stiffness.

In terms of elastic recuperation, Figure 5 presents its evolution with the impacts number, where the last impact is not represented because it occurs full penetration (Elastic energy = 0). The elastic energy was calculated as the difference between the absorbed energy and the energy at peak load, and N is the number of impacts at any given instant of the test and N_f is the number of impacts to failure. For each condition studied a curve is presented, however, they are representative of all curves obtained for each configuration.

FIGURE 5

As expected, the elastic energy decreases with the increasing of impacts number and this trend shows to be very dependent on the distance. These curves agree with the literature [**42, 43**] and, except for the control samples and for the distance of 20 mm, the data can be fitted by a polynomial of order two. This means that the damage occurs immediately after the first impact and its evolution is very fast after that. On the other hand, for the control samples and for the distance of 20 mm, the data can be fitted by a polynomial of order three, where the different stages observed are consequence of damage accumulation [**39**]. Relatively to the control samples, for example, the elastic recuperation decreases around 18.8% during the first 25% of the total life, followed by a slow decreasing during the second stage. Finally, in the third stage, the elastic energy drops suddenly. For the distance of 20 mm, the first stage decreases only 13.8% as consequence of the damage severity promoted by the first impacts. As discussed previously, the stress concentration associated with the lower stiffness of the sample promoted by the hole is responsible by higher damages and, consequently, lower elastic energy.

After appearing the first cracks (stage I), the second stage is characterized by the propagation/multiplication of the cracks with the number of impacts, until a saturation occurs. The cracks initiated at the point of impact propagate towards the hole, whereas the other cracks initiated near the hole edge propagate towards the impact centre. Finally, the saturation promotes a rapid acceleration

of the damage, accompanied by new damage mechanisms, up to to the final failure. In the third stage the damage is characterised by the failure of fibres. On the other hand, when the second stage is absent (samples characterized by a second order polynomial), all these damage mechanisms occur, but much more rapidly.

In terms of impact bending stiffness, its evolution with the impacts number is shown in Figure 6. These data correspond to the same tests shown in Figure 5. It is possible to observe that, for each configuration, these curves and the ones shown in Figure 5 present a similar behaviour. Simultaneously, comparing the first value of the IBS for the different configurations, it is possible to observe that the presence of the hole and its distance to the impact point affects significantly the stiffness of the sample. Comparatively to the control samples, and for the first impact, the IBS decreases about 9.8%, 19.7%, 31.7% and 38.2% for the distances of 20 mm, 10 mm, 5 mm and 0 mm, respectively. Therefore, the impact bending stiffness can be correlated directly with the global damage, as suggested by Amaro *et al.* [**41**], and this parameter is able to assess the damage progression.

FIGURE 6

Figure 7 shows the evolution of the damages with the multi-impacts for the distance of 20 mm (Figure 7a) and for the distance of 0 mm (Figure 7b). These configurations were selected because they represent different damage profiles, as discussed in the last paragraphs. The visual damages are in good agreement with the described previously.

FIGURE 7

Finally, Figures 8 and 9 show the repeated impacts effect on the maximum load and maximum displacement, respectively. One more time, the dimensionless format was used for clarity.

FIGURE 8

FIGURE 9

It is possible to observe that the maximum load tends to decrease, following the same tendency observed previously for the other parameters (elastic recuperation and IBS). For the control laminates and for the distance of 20 mm there are three stages, whereas for the other configurations this parameter

follows a polynomial of order two. One more time, the number of stages is related with the damage severity introduced by hole in terms of stress concentration and lower stiffness of the samples. When the fibre breakage begins, the maximum load drops dramatically because the local stiffness, at the point of impact, decreases significantly [**44**]. In terms of maximum displacement, Figure 8 shows an opposite trend.

4. CONCLUSIONS

The effect of the distance between the impact point and the hole on the impact **fatigue** strength of glass fibre/epoxy laminates was studied. **It was observed a significant influence on the fatigue life, where, comparatively to the control samples, a decrease of about 10.9%, 40%, 63.6% and 69.1% was observed for the distances of 20 mm, 10 mm, 5 mm and 0 mm, respectively. In terms of impact parameters, higher distances promote higher maximum loads and elastic restitution, but an opposite trend in terms of maximum displacement.** In terms of multi impacts, and for all configurations, a decreasing of the elastic energy can be found as consequence of damage accumulation. Moreover, the damage outline is also altered due to the presence of holes.

Finally, the projected damaged area was estimated by observation in counter-light and by ultrasonic C-scan. Independently of these techniques produce only a two-dimensional view of the damage zone, giving no through-thickness data, the first one shows to be a good alternative to characterize the damage in a global perspective.

References

[1] Green BG, Wisnom MR, Hallett SR. An experimental investigation into the tensile strength scaling of notched composites. Compos Part A Appl S 2007; 38: 867-78.

[2] Moure MM, Otero F, García-Castillo SK, Sánchez-Sáez S, Barbero E, Barbero EJ. Damage evolution in open-hole laminated composite plates subjected to in-plane loads. Compos Struct 2015; 133: 1048-57.

[3] Erçin GH, Camanho PP, Xavier J, Catalanotti G, Mahdi S, Linde P. Size effects on the tensile and compressive failure of notched composite laminates. Compos Struct 2013; 96: 736-44.

[4] Pandita SD, Nishiyabu K, Verpoest I. Strain concentrations in woven fabric composites with holes. Compos Struct 2003; 59: 361-68.

[5] Toubal L, Karama M, Lorrain B. Stress concentration in a circular hole in composite plate. Compos Struct 2005; 68: 31-6.

[6] Dai S, Cunningham PR, Marshall S, Silva C. Open hole quasi-static and fatigue characterisation of 3D woven composites. Compos Struct 2015; 131: 765-74.

[7] Achard V, Bouvet C, Castanié B, Chirol C. Discrete ply modelling of open hole tensile tests. Compos Struct 2014; 113: 369-81.

[8] Zitoune R, Crouzeix L, Collombet F, Tamine T, Grunevald Y-H. Behaviour of composite plates with drilled and moulded hole under tensile load. Compos Struct 2011; 93: 2384-91.

[9] Waas A, Babcock Jr CD. Observation of the initiation and progression of damage in compressively loaded composite plates containing a cutout. NASA Progress Report, 1986.

[10] Soutis C, Fleck NA. Static compression failure of carbon fibre T800/924C composite plate with a single hole. J Compos Mater 1990; 24: 536-58.

[11] Saha M, Prabhakaran R, Waters Jr WA. Compressive behavior of pultruded composite plates with circular holes. Compos Struct 2004; 65: 29-36.

[12] Suemasu H, Takahashi H, Ishikawa T. On failure mechanisms of composite laminates with an open hole subjected to compressive load. Compos Sci Technol 2006; 66: 634-41.

[13] Roy T, Chakraborty D. Delamination in FRP laminates with holes under transverse impact. Mater Des 2008; 29: 124–32.

[14] Adams R.D. and Cawley P.D. A Review of defects types and Non-Destructive Testing Techniques for composites and bonded joints. NDT Int 1998; 21: 208-222.

[15] Amaro A.M., Reis P.N.B., de Moura M.F.S.F. and Santos J.B. Damage detection on laminated composite materials using several NDT Techniques. Insight 2012; 54: 14-20.

[16] Davies GAO, Hitchings D, Zhou G. Impact damage and residual strengths of woven fabric glass/polyester laminates. Compos Part A-Appl S 1996; 27: 1147-56.

[17] de Moura MFSF, Marques AT. Prediction of low velocity impact damage in carbon–epoxy laminates. Compos Part A-Appl S 2002; 33: 361-8.

[18] Amaro AM, de Moura MFSF, Reis PNB. Residual strength after low velocity impact in carbon–epoxy laminates. Mater Sci Forum 2006; 514-516: 624-8.

[19] Amaro AM, Reis PNB, de Moura MFSF. Delamination effect on bending behaviour in carbon–epoxy composites. Strain 2011; 47: 203-8.

[20] Reis PNB, Ferreira JAM, Antunes FV, Richardson MOW. Effect of interlayer delamination on mechanical behavior of carbon/epoxy laminates. J Compos Mater 2009; 43: 2609-21.

[21] Green ER, Morrison CJ, Luo RK. Simulation and experimental investigation of impact damage in composite plates with holes. J Compos Mater 2000; 34: 502-21.

[22] Luo RK. The evaluation of impact damage in a composite plate with a hole. Compos Sci Technol 2000; 60: 49-58.

[23] Amaro AM., Reis PNB, de Moura MFSF, Neto MA. Influence of open holes on composites delamination induced by low velocity impact loads. Compos Struct 2013; 97: 239-44.

[24] Abrão AM., Campos Rubio JC, Faria PE, Davim JP. The effect of cutting tool geometry on thrust force and delamination when drilling glass fibre reinforced plastic composite. Mater Des 2008; 29: 508-13.

[25] Khashaba UA., El-Sonbaty IA, Selmy AI, Megahed AA. Machinability analysis in drilling woven GFR/epoxy composites: Part I - Effect of machining parameters. Compos Part A-Appl S 2010; 41: 391-400.

[**26**] Amaro AM., Reis PNB, Magalhaes AG, de Moura MFSF. The Influence of the boundary conditions on low-velocity impact composite damage. Strain 2011; 47: E220-26.

[**27**] Belingardi G, Vadori R. Low velocity impact tests of laminate glass-fiber-epoxy matrix composite material plates. Int J Impact Eng 2002; 27: 213-29.

[**28**] Reis PNB, Ferreira JAM, Zhang ZY, Benameus T, Richardson MOW. Impact strength of composites with nano-enhanced resin after fire exposure. Compos Part B-Eng 2014; 56: 290-5.

[**29**] Schoeppner GA, Abrate S. Delamination threshold loads for low velocity impact on composite laminates. Compos Part A-Appl S 2000; 31: 903–915.

[**30**] Reis PNB, Ferreira JAM, Santos P, Richardson MOW, Santos JB. Impact response of kevlar composites with filled epoxy matrix. Compos Struct 2012; 94: 3520-28.

[**31**] Río TG, Zaer R, Barbero E, Navarro C. Damage in CFRPs due to low velocity impact at low temperature. Compos Part B-Eng 2005; 36: 41-50.

[**32**] Reis PNB, Ferreira JAM, Zhang ZY, Benameur T, Richardson MOW. Impact response of kevlar composites with nanoclay enhanced epoxy matrix. Compos Part B-Eng 2013; 46: 7-14.

[33] Durão LMP, Tavares JMRS, Albuquerque VHC, Gonçalves DJS. Damage evaluation of drilled carbon/epoxy laminates based on area assessment methods. Compos Struct 2013; 96: 576-83.

[**34**] Schrauwen B, Peijs T. Influence of matrix ductility and fibre architecture on the repeated impact response of glass-fibre-reinforced laminated composites. Appl Compos Mater 2002; 9: 331–352.

[**35**] Boukhili R, Bojji C, Gauvin R. Fatigue mechanisms under low energy repeated impact of composite laminates. J Reinf Plast Compos 1994; 13: 856-870 .

[**36**] Whitney JM, Nuismer RJ. Stress fracture criteria for laminated composites containing stress concentrations. J Compos Mater 1974; 8: 253-65.

[**37**] Nuismer RJ, Whitney JM. Uniaxial failure of composite laminates containing stress concentrations. Fracture mechanics of composites ASTM STP 593, 1975: p. 117.

[**38**] Amaro AM, Reis PNB, de Moura MFSF, Santos JB. Influence of the specimen thickness on low velocity impact behavior of composites. J Polym Eng 2012; 32: 53-8.

[**39**] Amaro AM, Reis PNB, de Moura MFSF, Neto MA. Influence of multi-impacts on GFRP composites laminates. Compos Part B-Eng 2013; 52: 93- 99.

[**40**] David-West OS, Nash DH, Banks WM. An experimental study of damage accumulation in balanced CFRP laminates due to repeated impact. Compos Struct 2008; 83: 247-58.

[**41**] Amaro AM, Reis PNB, Neto MA, Louro C. Effects of alkaline and acid solutions on glass/epoxy composites. Polym Degrad Stabil 2013; 98: 853-62.

[**42**] Azouaoui K, Rechak S, Azari Z, Benmedakhene S, Laksimi A, Pluvinage G. Modelling of damage and failure of glass/epoxy composite plates subject to impact fatigue. Int J Fatigue 2001; 23: 877-85.

[**43**] Amaro AM, Reis PNB, Neto MA, Cirne JM. Residual impact strength of carbon/epoxy laminates after flexural loadings. Compos Struct 2016; 146: 69-74.

[**44**] Schrauwen B, Peijs T. Influence of matrix ductility and fibre architecture on the repeated impact response of glass-fibre-reinforced laminated composites. Appl Compos Mater 2002; 9: 331–352.

Figures

Figure 1 - Geometry of the samples, dimensions in mm (d = 0, 5, 10 and 20 mm).

Figure 2 - Load-time and energy-time curves: a) Obtained for the first impact on control samples and for the distances of 10 mm and 0 mm; b) Showing the typical evolution of the curves for the control samples subjected to multi-impacts.

Figure 3 - Damages obtained after the first impact for: a) Control samples; b) Samples with the hole distanced 10 mm from the impact point.

Figure 4 - Effect of the distance between the impact point and hole on the impact strength.

Figure 5 - Elastic recuperation versus N/N_f.

Figure 6 - Impact bending stiffness versus N/N_f.

Figure 7 - Damages for different number of impacts: a) Samples tested for a distance of 0 mm; b) Samples tested for a distance of 20 mm.

Figure 8 - Maximum impact load versus N/N_f.

Figure 9 - Maximum displacement versus N/N_f.

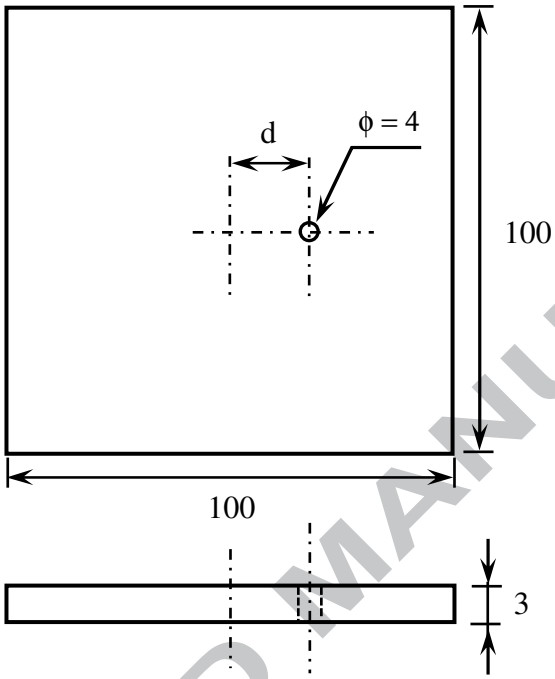

Figure 1 - Geometry of the samples, dimensions in mm (d = 0, 5, 10 and 20 mm).

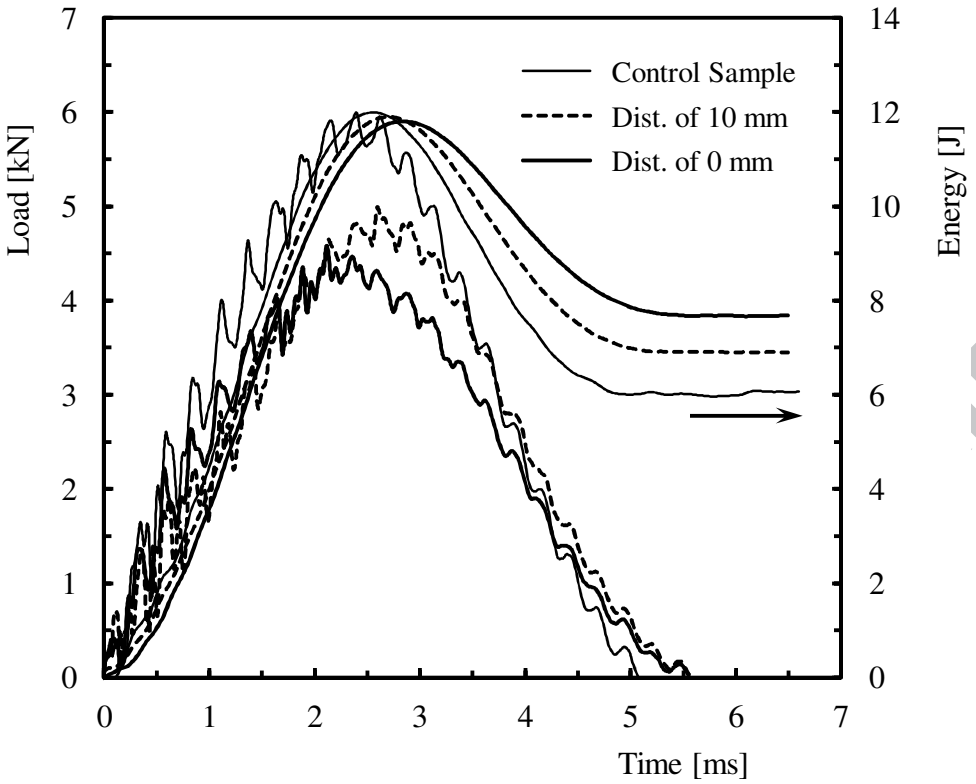

a)

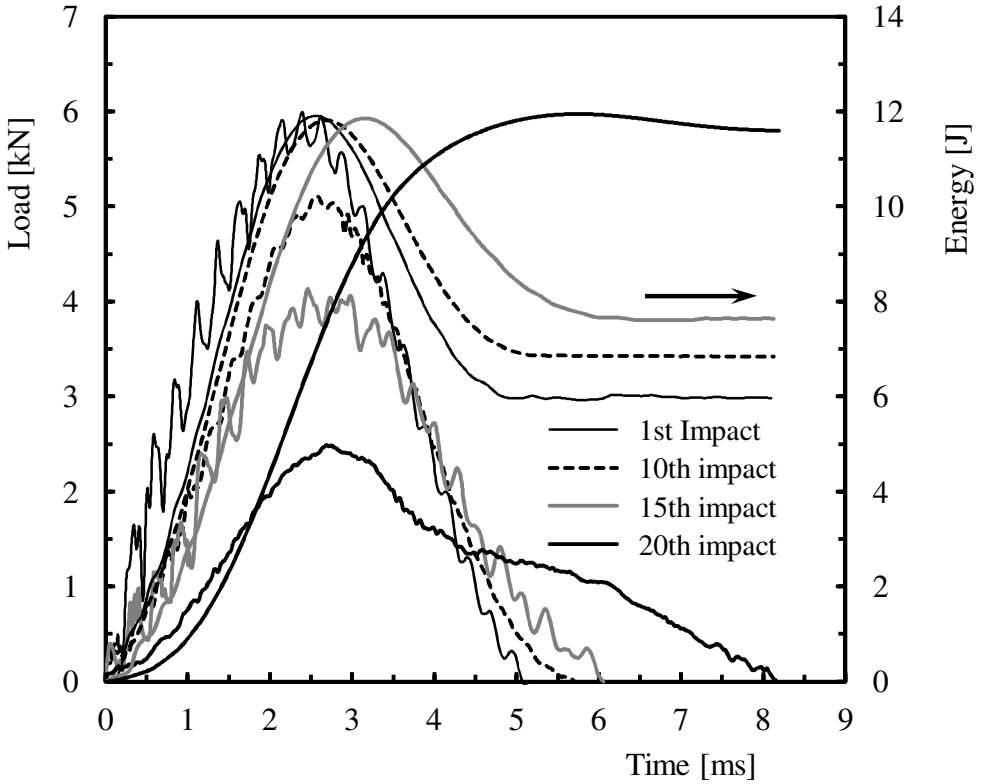

b)

Figure 2 - Load-time and energy-time curves: a) Obtained for the first impact on control samples and for the distances of 10 mm and 0 mm; b) Showing the typical evolution of the curves for the control samples subjected to multi-impacts.

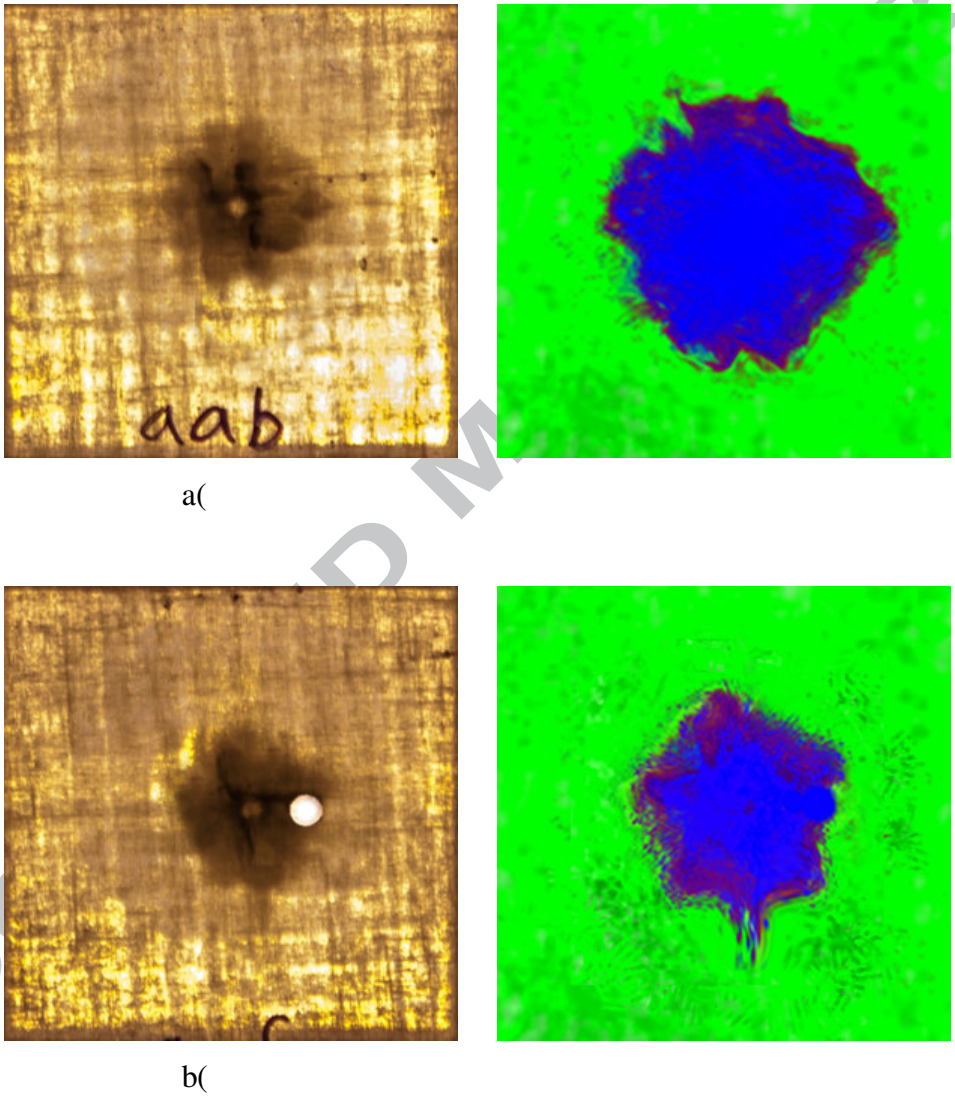

a(

b(

Figure 3 - Damages obtained after the first impact for: a) Control samples; b) Samples with the hole distanced 10 mm from the impact point.

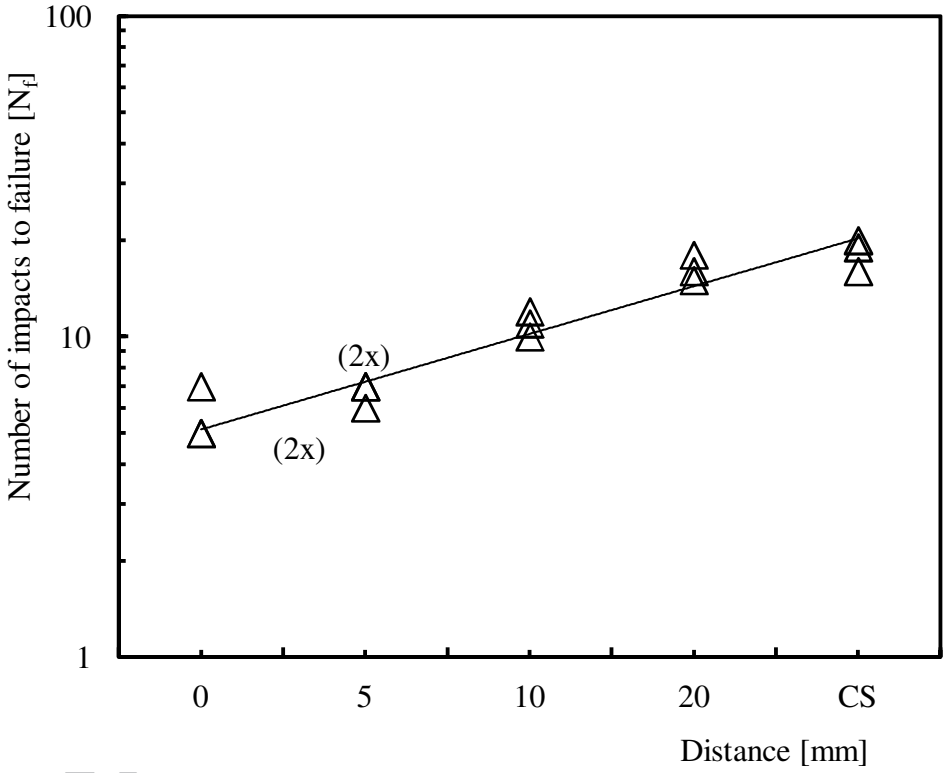

Figure 4 - Effect of the distance between the impact point and hole on the impact strength.

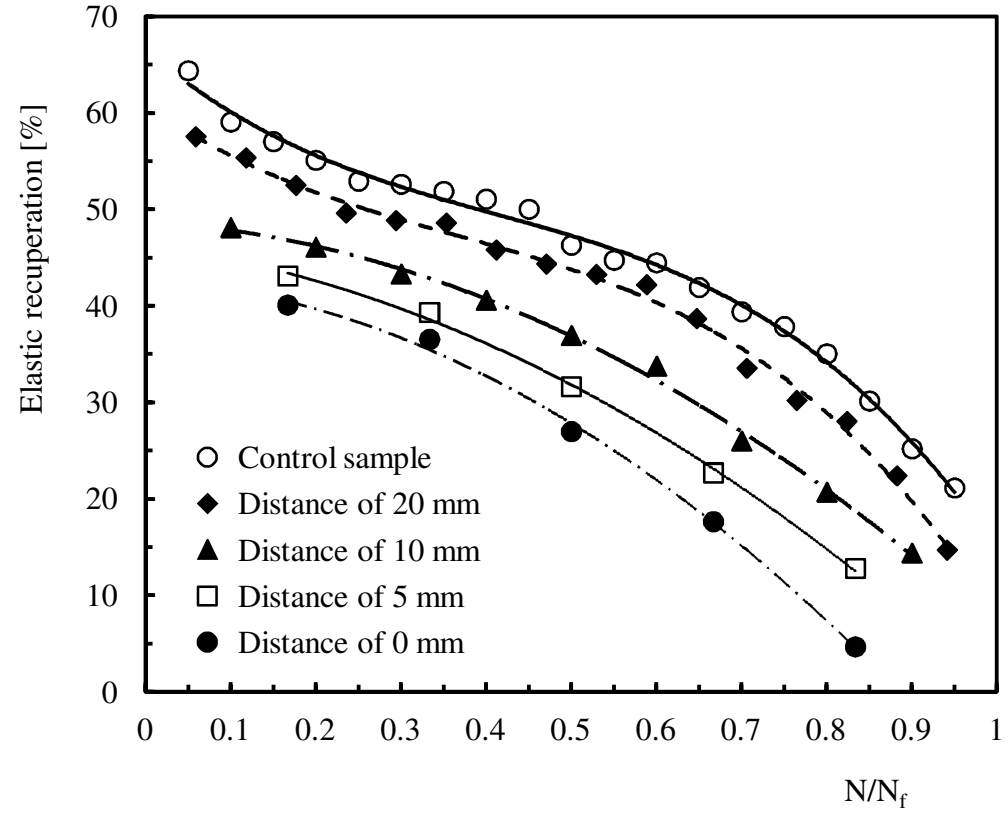

Figure 5 - Elastic recuperation versus N/N_f.

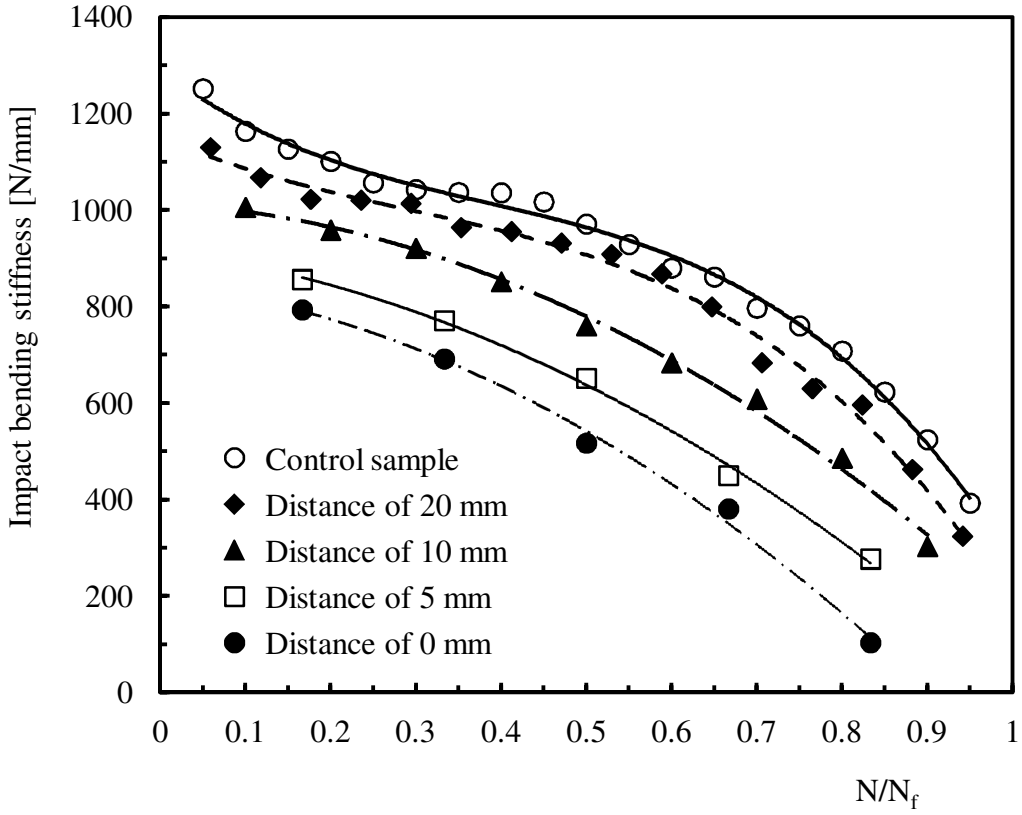

Figure 6 - Impact bending stiffness versus N/N_f.

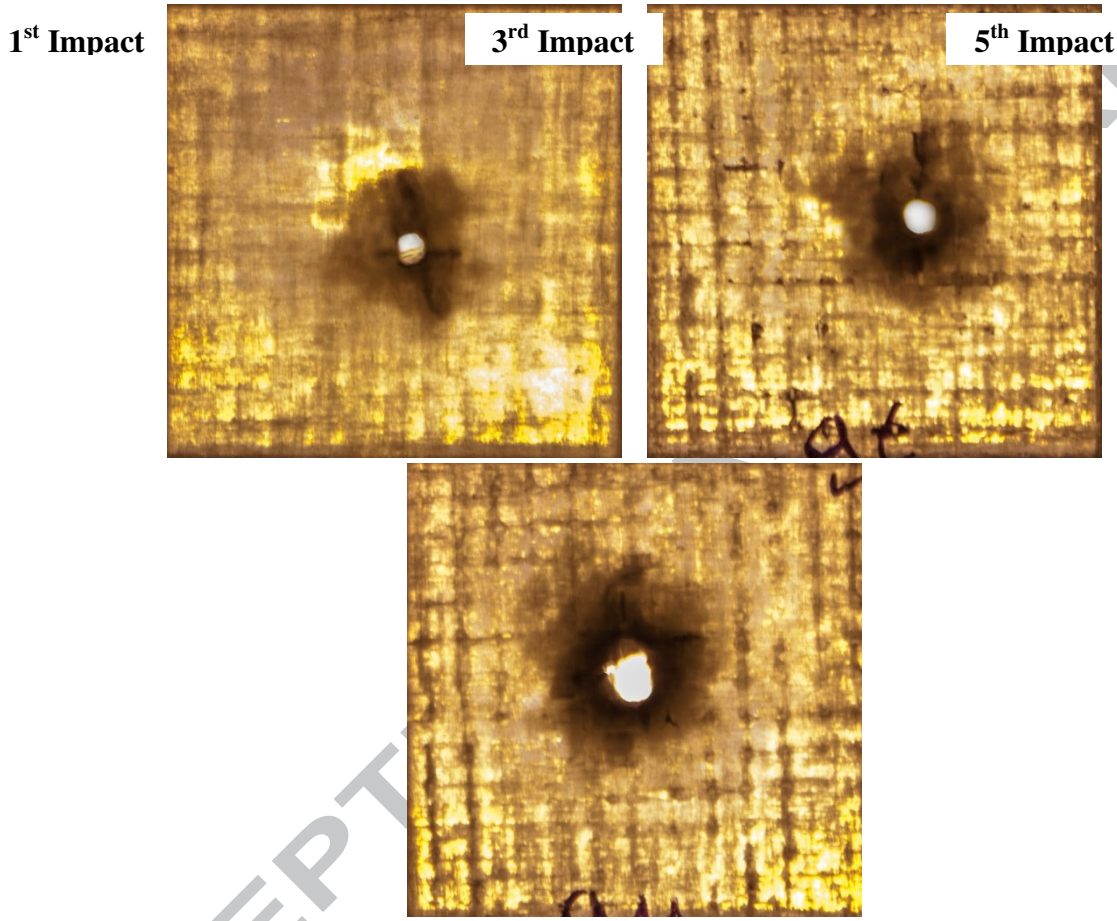

a)

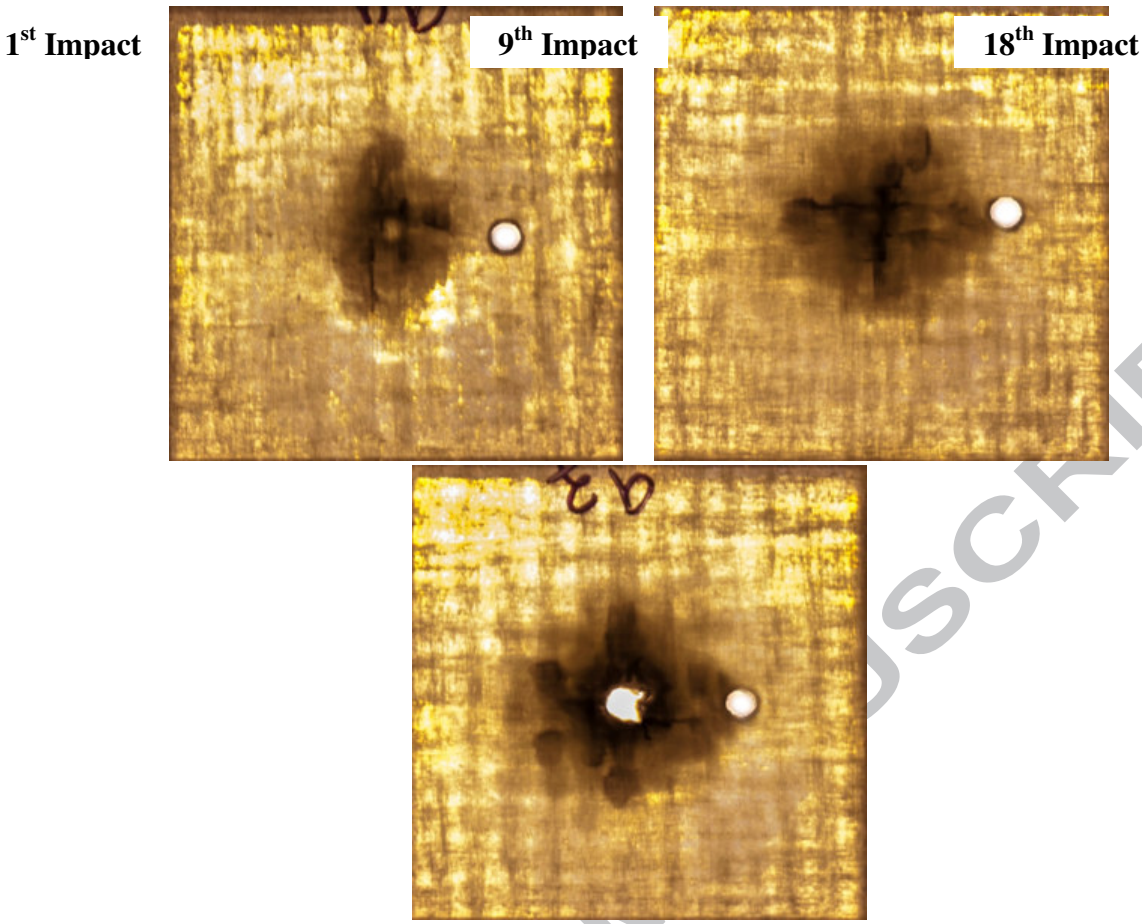

Figure 7 – Damages for different number of impacts: a) Samples tested for a distance of 0 mm; b) Samples tested for a distance of 20 mm.

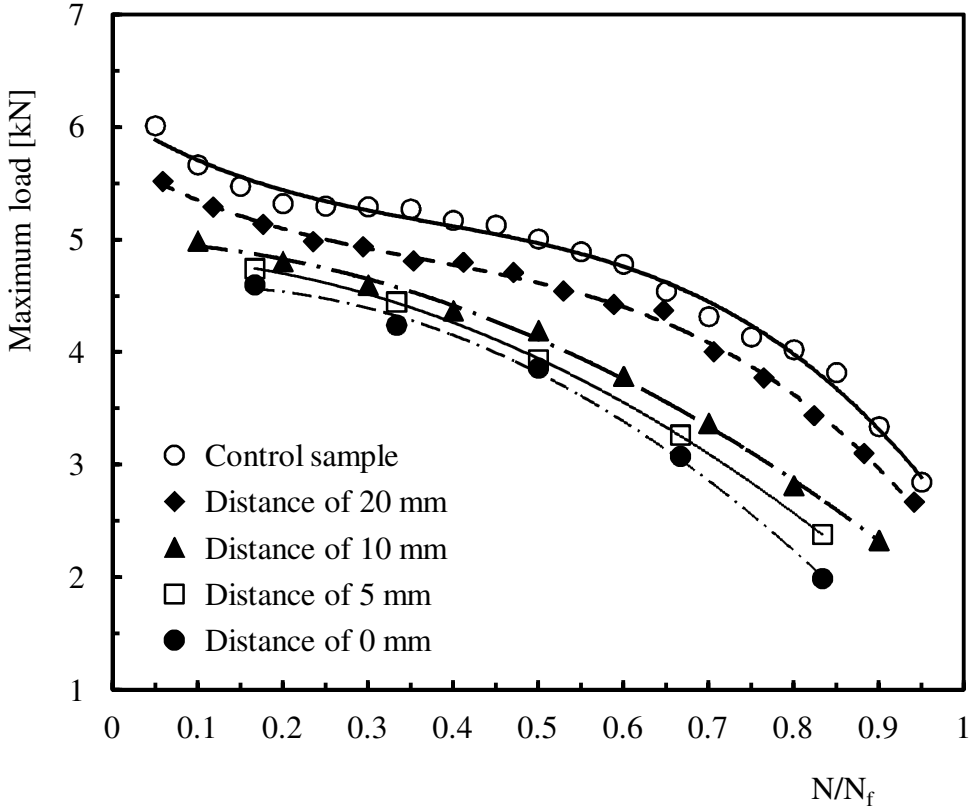

Figure 8 - Maximum impact load versus N/N_f.

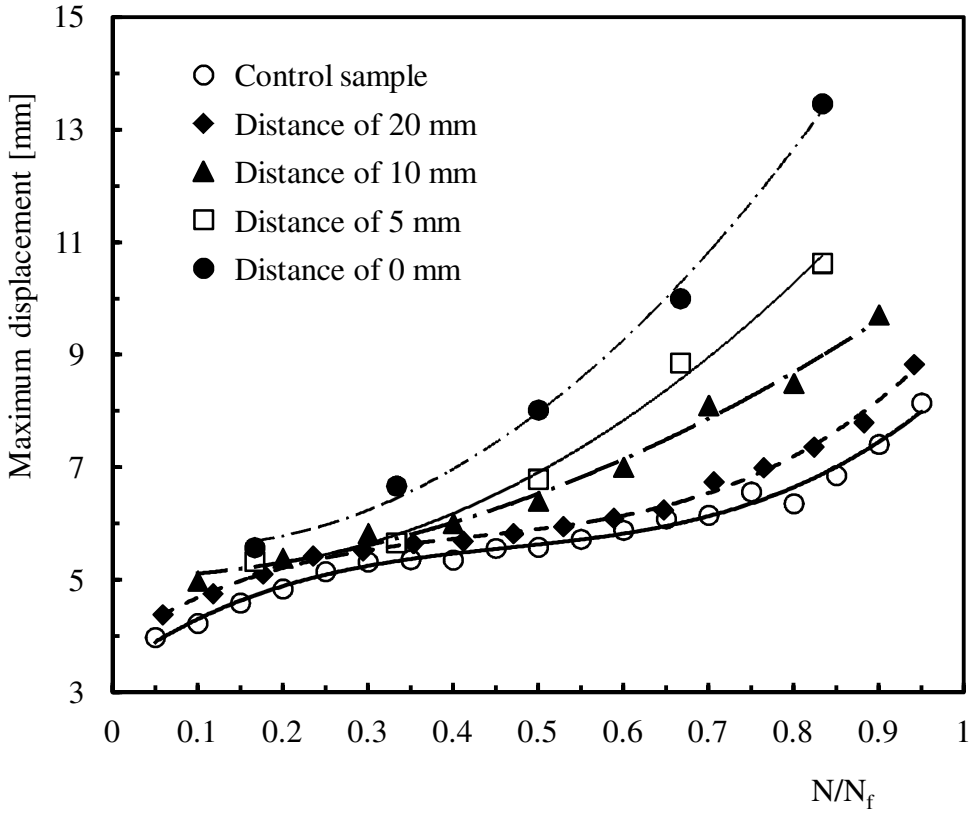

Figure 9 - Maximum displacement versus N/N_f.

Tables

Table 1 – Parameters obtained from the first impact.

Table 1 – Parameters obtained from the first impact.

Distance [mm]	Average values for the first impact					
	P_{max} [kN]	SD [kN]	Displ. [mm]	SD [mm]	ER [%]	SD [%]
CS	5.90	0.11	4. 1	0.1	65.7	1.4
0	4.59	0.04	5,7	0.3	40.4	0.2
5	4.78	0.12	5.3	0.2	43.2	0.5
10	4.99	0.16	5.0	0.1	47.6	0.4
20	5.54	0.07	4.4	0.1	59.2	0.9